# STEADY STATE PERFORMANCE OF SWITCHED RELUCTANCE GENERATOR

Hany. M..Hasanien.
Electrical Power and Machines Dept., Faculty of Engineering, Ain-shames University, Cairo, Egypt.
Hanies50@yahoo.com

**ABSTRACT**

***This paper presents the steady state operation of the switched reluctance generator (SRG). The performance of the generator is studied under constant speed operation and different values of both the switching turn-on and off angles. The turn-on and turn-off angles are the two parameters through which we can control the electric power generation. The response of the generator is obtained at low and high speed in order to illustrate the performance of the generator. Also, this paper presents a PI controller in order to control the power of SRG under constant voltage operation. The dynamic response of the generator is studied under different values of controller parameters for both low and high speed operation. The effectiveness of the proposed controller is then obtained.***

## 1. INTRODUCTION

The switched reluctance generator is a doubly salient, singly-excited generator as shown in Fig 1. It has unequal number of salient poles on both the rotor and the stator, but only one member (usually the stator) carries windings, and each two diametrically poles usually form one phase. The rotor has no winding, magnets, or cage winding and is built up from a stack of salient-pole lamination. So it is considered as a simple and robust construction machine [1-3].

Fig. 2 illustrates a four-phase SRG converter system with two controllable power semiconductor switches and two diodes per phase that sources a resistive load. The filter capacitor *C* is chosen large enough to assure fairly constant *dc*-link voltage at each stroke.

Thus each phase has a pulse nature parameters (current, flux-linkage, and torque). The torque is produced by the tendency of the rotor poles to align with the stator poles of the excited phase, and it is independent of the current phase direction.

The SRG possesses many inherent advantages such as simplicity, robustness, low manufacturing cost, high speed, and high efficiency [4]. The SRG is under development for variable speed applications. To date, these applications include sourcing aerospace power systems [5], hybrid vehicles [6], and wind turbine applications [7,8]. The aerospace and automotive applications are generally characterized by high speed operation. The wind energy application is characterized by low speed, high torque operation.

## 2. STATIC CHARACTERISTICS

The model of an SRG for dynamic analysis comprises the set of phase circuit and mechanical differential equations. In integerating these equations, the problem centers on handling the data (flux-linkage/angle/current) used to describe the magnetic nature of the switched reluctance machine. Different methods have been used for numerical integeration of the nonlinear differential equations of the SRG with the magnetization data in the form of a look-up table $\psi(\theta,i)$ [9,10]. The integeration of these equations to obtain the waveforms of phase current and torque against time requires the definition of magnetic behavior of the switched reluctance machine in the form of look-up tables $i(\theta,\psi)$ and $T(\theta,i)$ to enable the values of current and torque of each phase to be updated after each step of numerical integeration.

## 3. REPRESENTATION OF THE MAGNETIC CURVES OF SRG

There are different methods used to represent the magnetization curves of SRG. In the first

method a mathematical function of the measured flux-linkage points versus rotor angle at fixed stator current values is obtained, this function has the polynomial form:

$$\Psi(\theta) = a_o + a_1(\theta) + a_2(\theta)^2 + \text{------} + a_k(\theta)^k \quad (1)$$

Where $a_o$ , $a_1$ , $a_2$ , ------ , $a_k$ are the polynomial coefficients and they are determined using the least square error method, θ is the rotor angle in electrical degrees. For p values of current the following set of polynomials could be obtained as:

$$\Psi_b(\theta) = a_{ob} + a_{1b}(\theta) + \text{---------} + a_{kb}(\theta)^k \quad (2)$$

Where b=1,2,----p, and any one set of coefficient $a_{ob}$ , $a_{1b}$ ,---- $a_{kb}$ is independent of the chosen current. Equation (2) gives the flux-linkage at p discrete values of current and in order to represent the flux-linkage at any current the sets of coefficients $a_{01}$ , $a_{02}$ , ------$a_{0p}$ ; $a_{11}$ , $a_{12}$ , ------ $a_{1p}$ ; $a_{21}$ , $a_{22}$ , ------$a_{2p}$ ; $a_{k1}$ , $a_{k2}$ , ------$a_{kp}$ should be replaced by polynomials of jth order in terms of current [9,10]. So the general expression for the flux-linkage as a function of both current and rotor position is:

$$\Psi = \sum_{b=0}^{k} (A_{ob} + A_{1b}.i + \text{------} A_{jb} . (i)^j ). \ \theta^b \quad (3)$$

In method 2 an exponential function is used to represent the magnetization curves of the SRG because these functions are a natural fit to typical magnetization curves. The used exponential function consists of three exponential terms in addition to a linear one.

$$\Psi = a_0 i + a_1(1-e^{-\alpha 1 i}) + a_2(1-e^{-\alpha 2 i}) + a_3(1-e^{-\alpha 3 i}) \quad (4)$$

Where $a_0$, $a_1$, $a_2$, $a_3$ are coefficients and $\alpha_1$, $\alpha_2$, $\alpha_3$ are constants. A nonlinear least square analysis is used to obtain each of the coefficients, then the Ψ/I curves are obtained at a constant measured rotor angle for each curve, and linear interpolation between coefficients and rotor angle is used to determine the intermediate curves of Ψ/I.

In method 3 the data defining the magnetic nature of the machine are stored as a look-up table to represent the function Ψ(θ,I) which has been formed from a set of measured curves, and a quadratic interpolation is used to get the intermediate values of flux-linkage for each curve because it has been found that this function is suitable to represent the saturated part. It is important to obtain the table of I(θ,Ψ) while integrating the motor equations, this table is obtained by inverting the table of Ψ(θ,I), and is formed at sufficient number of equally spaced angles and flux-linkages. The values of $I(\Psi)|_{\theta=\text{constant}}$ at equally spaced flux-linkages are found using quadratic interpolation and $I(\Psi)|_{\theta=\text{constant}}$ is represented by the equation:

$$I(\theta,\Psi) = A\,\Psi^2 + B\,\Psi + C \quad (5)$$

At least the parameters of three points are necessary to determine the coefficients (A,B,C) of equation (5).

Method 4 is used to represent the flux-linkage current curves of the SRG using the measured data. This method (which has been adopted in this paper) is carried out using the Cubic Spline Interpolation technique, which is more accurate than the other methods and gives more smoothed representation of the magnetization curves.

After getting the magnetization curves of the SRG, the static torque characteristics can be obtained in order to get the whole static characteristics of the generator. The static torque characteristics are plotted against rotor angle for different values of current.

The static torque is computed by numerical differentiation of the co-energy which in turn is computed by numerical integration of the flux-linkage current curves.

$$W'(\theta, i) = \int_0^i \Psi(\theta, i)\,di \Big|_{\theta=\text{const}} \quad (6)$$

$$T(\theta, i) = \frac{\partial W'(\theta, i)}{\partial \theta}\Big|_{i=\text{const}} \quad (7)$$

The used method in this study is based on some input curves obtained by measurement

## 4. COMPUTATION OF THE STATIC CHARACTERISTICS

The magnetization characteristics are extended using the cubic spline interpolation algorithm to cover the interval of rotor angles between the unaligned and the aligned positions as shown in Fig 3. The co-energy curves are calculated from equation (6) by applying the trapezoidal rule in numerical integration. The static torque curves of the SRG are computed according to equation (7) using numerical differentiation.

The previous characteristics data are stored as a look-up table. Thus there are two look-up tables for the flux-linkage and for the static torque characteristics available to use during the computation of the generator differential equations.

The computed torque as a function of the current and rotor angle is illustrated in Fig 4. The computations are carried out at different rotor angles between the aligned position (60º) and the unaligned position (90º), which forms half the rotor pole-pitch.

## 5. SRG PERFORMANCE UNDER CONSTANT SPEED OPERATION

To predict the generator performance, it is necessary to solve the differential equations for the appropriate switched conditions, and an additional mechanical equation for a variable speed. It is valuable to note that the electromagnetic nature of the generator is reflected in the variation of the phase winding inductances with the rotor displacement, where the mutual inductances with other phase windings are often very small and are neglected.

The phase equation of the generator has the general following formula:

$$\frac{d\Psi_k(\theta_k, i_k)}{dt} = \pm V - R\, i_K \qquad (8)$$

Where R is the phase winding resistance, Ψ is the flux-linkage as a function of current and rotor angle, and V is the applied voltage which is positive during the conduction period, and is negative from the switch-off angle until the extinction angle, and otherwise equals zero.

Thus,

$$\begin{aligned} V &= E \quad \text{when} \quad \theta on < \theta < \theta off \\ V &= -E \qquad\qquad \theta off < \theta < \theta ext \\ V &= 0 \qquad\qquad\quad \theta > \theta ext \end{aligned} \qquad (9)$$

Where E is the dc supply voltage

A switched reluctance machine operates in generating mode by retarding the fire-angles so that conduction period comes after the aligned position, where the phase inductance is decreasing, $dL/d\theta < 0$ . In such case, the energy returned to the *dc*-link during the de-fluxing period $P_o$ exceeds the excitation energy supplied during the dwell period $P_{exc}$ and the difference is provided by the prime mover. The electrical output power to the load is:[11]

$$P_{out} = P_o - P_{exc} \qquad (10)$$

Fig 5 shows the current, and torque curves at speed of 500 rpm, under switching-on angle θon=70º and switching-off angle θoff=80º, it can be noted that the dc electrical output power to the load $p_{out}$ =0.3 p.u. Fig 6 shows the current, and torque curves at speed of 500 rpm, under switching-on angle θon=65º and switching-off angle θoff=80º, it can be noted that the dc power $p_{out}$ will be 0.45 p.u due to the increasing of the conduction period.

It can be predicted that the switching-on angle (θon) must be at the aligned position (i.e60º) to permit the current to increase rapidly before the effect of the back emf which appears at the start of negative slope inductance.

Fig 7 shows the current, and torque curves at speed of 500 rpm, under switching-on angle θon=60º and switching-off angle θoff=80º, the dc power $p_{out}$ will be 0.75 p.u. When θoff is increased, the conduction period is increased. The dc power $p_{out}$ is increased to 1.2 p.u as shown in Fig 8.

It can be noted that the phase current will exceed its maximum allowable value (reference value which here the rated value). Thus, the chopping mode (PWM current-control) is clearly recommended for the low speed operation.

On the other hand, if the switching-on angle is beyond the aligned position, this will produce motoring torque due to the switching in the positive slope inductance. Also, if the switching-off angle is increased above 85º, the extinction angle is increased above 90º, and the current in this unaligned position will produce motoring torque, and these cases are avoided in studying the SRG performance.

Figs 9-12 show the current, and torque curves of the four phases SRG at speed of 1500 rpm, under different values of θon and θoff. The operation under high speed with angle control uses a single pulse mode

From the previous curves, it can be noted that the operation under high speed gives the advantages of using larger conduction period. But the induced back emf under large conduction period helps the phase current. Thus, the chopping mode (current-control) is clearly recommended for This case as shown in Figs 11,12. Therefore, there is smooth transition between single pulse mode of operation and PWM current control mode of operation. Wide pulse duration will increase the overlapping between the different phases which, in turn, increases the average power generated of the SRG.

## 6. POWER CONTROL OF SRG USING THE PI CONTROLLER

The proportional plus integral (PI) controller is one of the famous controllers that is used in a wide range in the industrial applications. The output of the PI controller in time domain, is defined by the following equation:-

$$V_c(t) = K_p\, e(t) + \frac{K_i}{T_i} \int_0^t e(t)\, dt \qquad (11)$$

Where:

$V_c(t)$ is the output of the PI controller, $K_p$ is the proportional gain, $K_i$ is the integral gain, $T_i$ is the integral time constant, and e(t) is the instantaneous error signal.

The system under study consists of a SRG fed from a DC supply via an inverter, as shown in Fig 13. The final output of the controller is used to regulate the switching-on angle of the SRG to control the generator power, while the input of the controller is the power deviation.

The generator power deviation (e), in p.u is given by the following equation:-

$$e = \frac{p_{ref} - p}{p_{ref}} \qquad (12)$$

Then, the new turn-on switching angle $\theta_{onnew}$, which is obtained from the controller output is calculated by the following equation:-

$$\theta_{onnew} = \theta_{onold} - [K_p\, e(t) + \frac{Ki}{Ti} \int_o^t e(t)\, dt\ ] \qquad (13)$$

Figs 14-16, show the obtained generator power of SRG using the proposed PI controller. It is noted that when the proportional gain $k_p$ increases, the conduction period increases. Also, the excitation power $P_{exc}$ is slightly increased, but the return back power $P_o$ is increased more and more. Therefore the average power given to the load $p_{out}$ is increased under low and high speed.

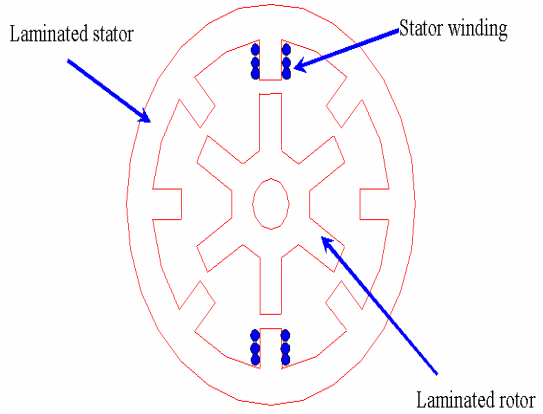


Fig 1. A cross section of a 4-phase, 8/6 SRG.

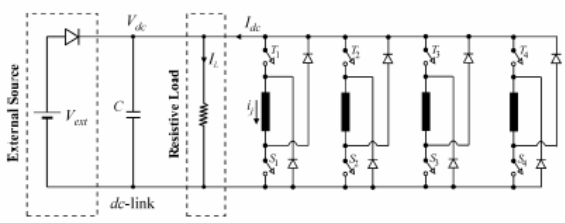


Fig 2. Generator system with four-phase SRG.

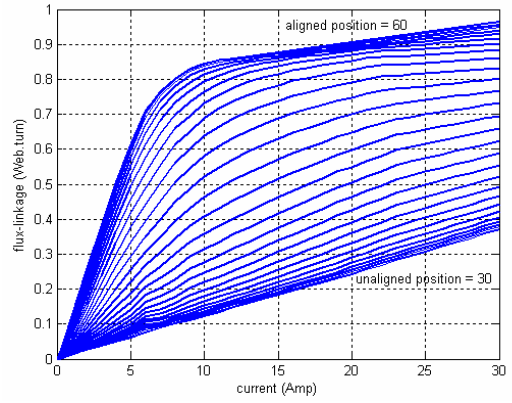


Fig 3. The phase flux-linkage as a function of current and rotor position.

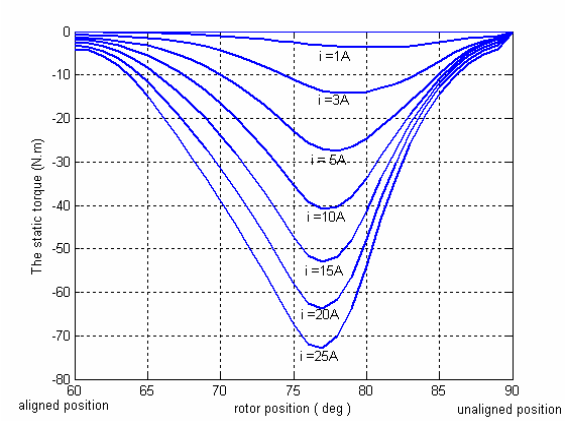


Fig 4. The static torque curves of SRG.

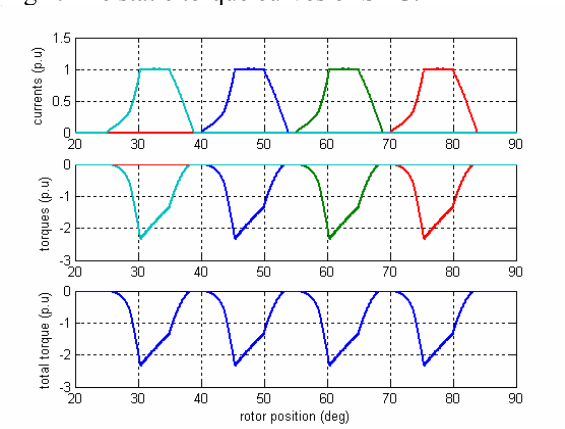


Fig 5. The generator performance at speed of 500rpm, θon = 70º and θoff = 80º. $T_{av}$ = -0.87 p.u, and $p_{out}$=0.3 p.u.

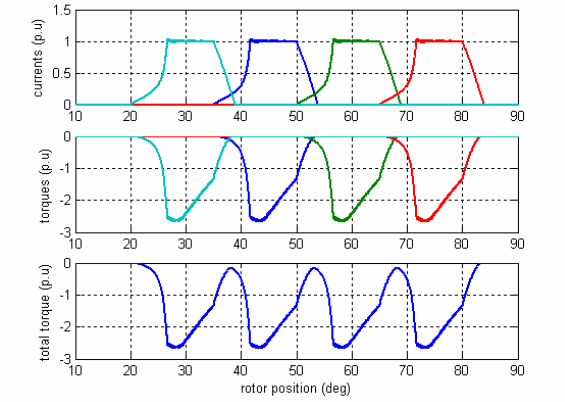


Fig 6. The generator performance at speed of 500rpm, θon = 65º and θoff = 80º. $T_{av}$ = -1.5 p.u, and $p_{out}$=0.45 p.u.

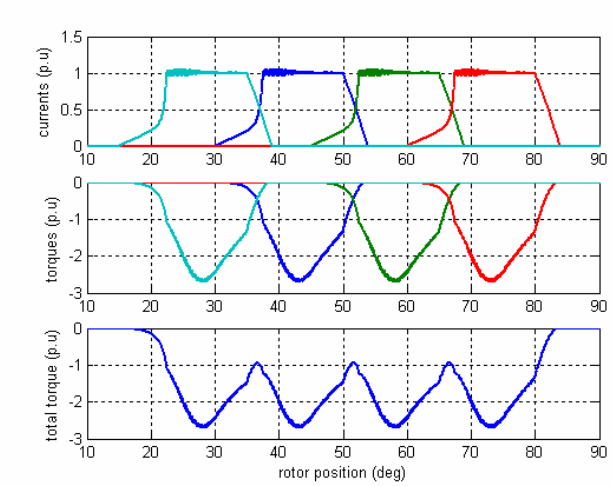


Fig 7. The generator performance at speed of 500rpm, θon = 60º and θoff = 80º. $T_{av}$ = -1.9 p.u, and $p_{out}$=0.75 p.u.

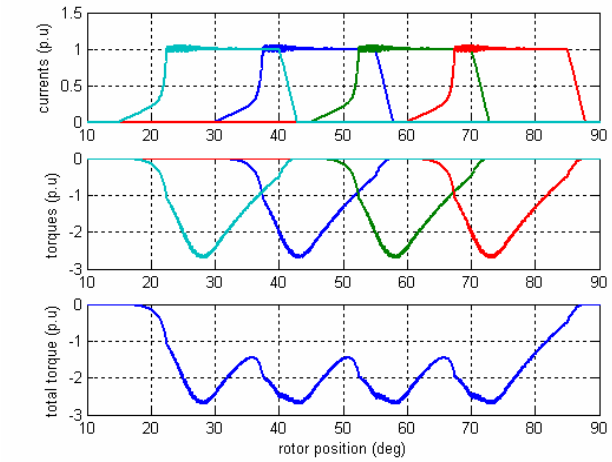


Fig 8. The generator performance at speed of 500rpm, θon= 60º and θoff = 85º. $T_{av}$ = -2.1 p.u, and $p_{out}$=1.2 p.u.

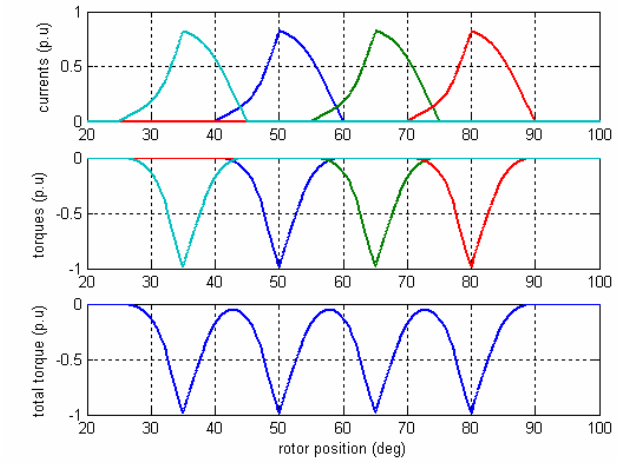


Fig 9. The generator performance at speed of 1500rpm, θon= 70º and θoff = 80º. $T_{av}$ = -0.38 p.u, and $p_{out}$=0.25 p.u.

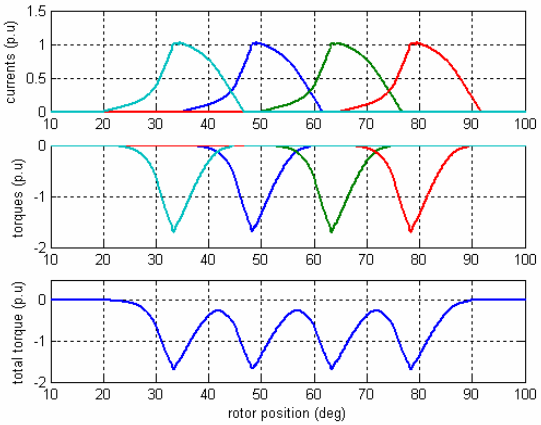


Fig 10. The generator performance at speed of 1500rpm, θon=65º and θoff = 80º. $T_{av}$ = -0.8 p.u, and $p_{out}$=0.4 p.u.

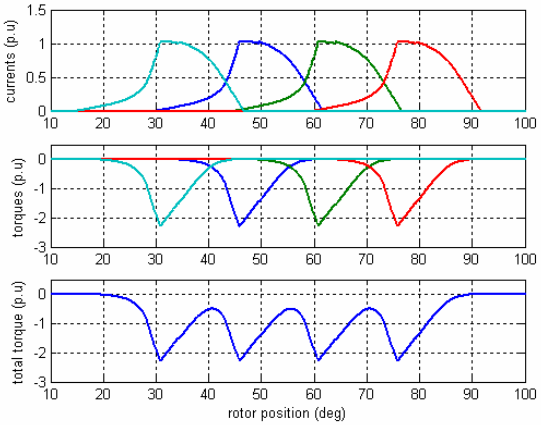


Fig 11. The generator performance at speed of 1500rpm, θon=60º and θoff = 80º. $T_{av}$ = -1.2 p.u, and $p_{out}$=0.6 p.u.

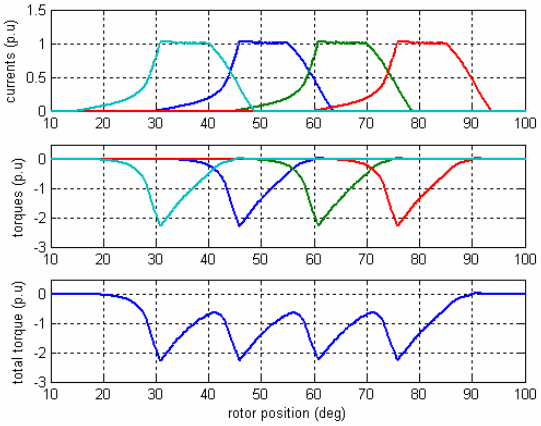


Fig 12. The generator performance at speed of 1500rpm, θon=60º and θoff = 85º. $T_{av}$ = -1.3 p.u, and $p_{out}$=1 p.u.

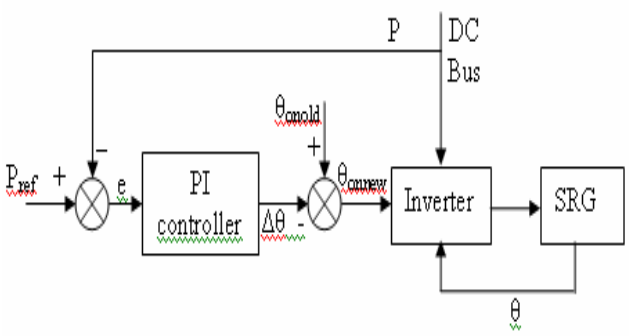


Fig 13. Structure of the controller for control SRG power.

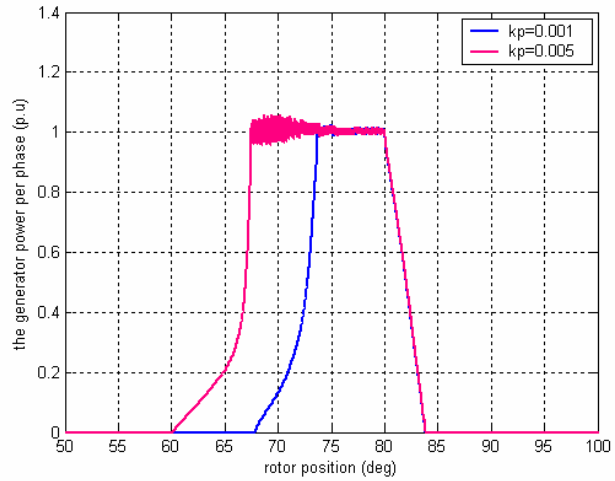


Fig. 14. The generator power curve under low speed of 500 r.p.m, $k_i$=0.005, V=360V, $\theta_{onold}$=70º, $\theta_{off}$=80º.

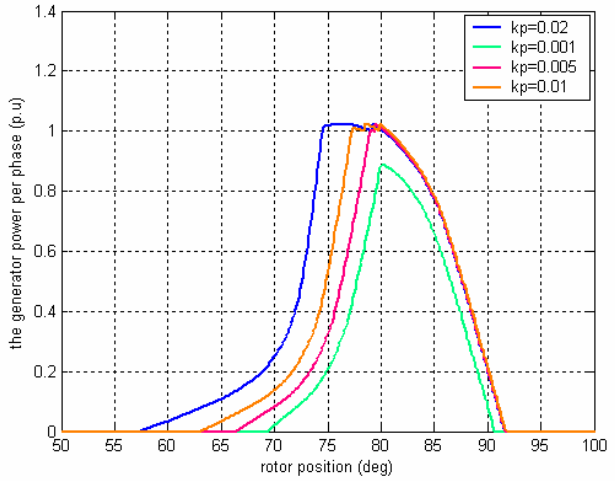


Fig. 15. The generator power curve under speed of 1500 r.p.m, $k_i$=0.005, V=360V, $\theta_{onold}$=70º, $\theta_{off}$=80º.

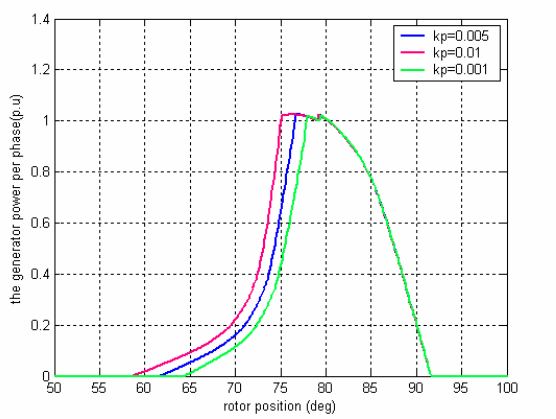


Fig. 16. The generator power curve under speed of 1500 r.p.m, $k_i$=0.005, V=360V, $\theta_{onold}$=65º, $\theta_{off}$=80º.

## 6. CONCLUSION

The cubic spline interpolation algorism is used to create the static characteristics of the switched reluctance generator. The performance of the generator under constant speed operation and different values of the switching on and off angles is studied. The switching-on angle, switching-off angle, and the phase current can control the electric power generated from the switched reluctance generator. Where, the chopped mode of control is recommended for low speed operation. Both of the chopped mode and pulse mode of control are recommended in the high speed operation according to the operating conditions. The operating conditions include the conduction period, and the dc output power generated.

Also, the PI controller is used to control the power of SRG under constant voltage operation. The dynamic response of the generator is studied under different values of controller parameters for both low and high speed operation. By inspection of the dynamic response, it can be realized that, The proposed controller can be used for increasing the output power generated.

## APPENDIX

The generator under study is a four phases, 8/6 SRG, the rated power is 4kw at 1500 rpm. The phase resistance is 0.1Ω, the machine inertia is 0.0012 kgm$^2$, the supply voltage=360V.

**REFERENCES**


[1] T. J. E. Miller,“ Switched reluctance motors and their control ”, Oxford University Press, 1993.

[2] P. J. Lawrenson, “ Variable speed switched reluctance motors ”, IEE Proc, Vol. 127, No. 4, pp. 253-265, 1980.

[3] Hany.M.Hasanien, N.H. Saad, M.A. Mostfa, M.A. Badr, “ Speed control of axial laminations switched reluctance motor provided with digital pole placement controller”, Proc. of the international conference on electrical machines (ICEM), pp. 376-380, 2006.

[4] D. A. Torrey, “ Switched reluctance generators and their control ”, IEEE Trans. on Industrial Electronics, Vol. 49, pp. 3-14, 2002.

[5] D. E. Cameron and J. H. Lang, “ The control of high speed variable reluctance generators in electric power systems ”, IEEE Trans. on Industry Applications, Vol. 29, pp. 1106-1109, 1993.

[6] J. M. Kokernak, D. A. Torrey and M. Kaplan, “ A switched reluctance starter/ alternator for hybrid electric vehicles ”, Power Electronics Proc ( PCIM) Conference, pp. 74-80, 1999.

[7] D. A. Torey, “ Variable reluctance generators in wind energy systems ”, *Proc. of the IEEE Power Electronics Specialists Conf.,* pp. 561-567, 1993.

[8] R. Cardenas, W. F. Ray and G. M. Asher, “ Switched reluctance generators for wind energy applications ”, *Proc. of the IEEE Power Electronics Specialists Conf.,* pp. 559-564, 1995.

[9] J. Corda, S. Masic, T. Mateljan, E. Skopljak, “Dynamic performance of a switched reluctance motor”, *proc. of the international Conference on Electrical Machines (ICEM)*, 1986.

[10] D.W.J. Pulle, “ New data base for switched reluctance drive simulation”, *IEE proceedings, B,* Vol. 138, NO. 6, 1991.

[11] Christos Mademlis and Iordanis Kioskeridis, “Calculation of the Optimal Fire Angles in Single-Pulse Controlled Switched Reluctance Generator Drives”, *Proc. of the international conference on electrical machines (ICEM),* pp. 161-166, 2006.